Tradeoffs Between Indoor Air Quality and Sustainability for Indoor Virus Mitigation Strategies in Office Buildings

Cary A. Faulkner¹ John E. Castellini Jr.¹ Yingli Lou² Wangda Zuo^{3,4} David M. Lorenzetti⁵ Michael D. Sohn⁵

Abstract

The COVID-19 pandemic has motivated building operators to improve indoor air quality (IAQ) through long-term sustainable solutions. This paper develops a modeling capability using the Modelica Buildings library to evaluate three indoor virus mitigation strategies: use of MERV 10 or MERV 13 filtration and supply of 100% outdoor air into a building with MERV 10 filtration. New evaluation metrics are created to consider the impact of improving IAQ on financial and environmental costs. The mitigation strategies are studied for medium office buildings in three locations in the United States with differing climates and electricity sources. The results show that use of 100% outdoor air can significantly improve IAQ with limited increases in costs in the milder climate, but leads to very high costs in the hot and humid and very cold climates. MERV 13 filtration can improve IAQ relative to MERV 10 filtration with small increases in costs in all locations. Keywords: Indoor air quality, costs, COVID-19, sustainability.

1 Introduction

Improving indoor air quality (IAQ) during the COVID-19 pandemic while limiting environmental impact in the age of rapid climate change is challenging. Operation of building heating, ventilation, and air-conditioning (HVAC) systems can mitigate indoor virus concentration and reduce risk of infection (Pease, Wang, et al. 2021; Shen et al. 2021; Vlachokostas et al. 2022; Pease, Salsbury, et al. 2022), but can also increase HVAC energy consumption (Faulkner et al. 2022; Cortiços and Duarte 2021). For example, higher outdoor air ventilation rates can increase heating/cooling energy usage, or use of efficient, high pressure drop filters can increase fan energy consumption. Improving IAQ while minimizing increases in energy costs and emissions is a challenge dependent on several factors, including mitigation strategy, climate, and electricity sources.

Previous literature studied tradeoffs between IAQ and HVAC energy consumption. Santos and Leal (Santos and

Leal 2012) examined the impact of increased ventilation rate on energy consumption in European cities. They found the increase in energy is dependent on climate and building type. Aviv et al. (Aviv et al. 2021) proposed a novel HVAC strategy to couple radiant systems and natural ventilation to increase outdoor air ventilation while minimizing energy consumption. Schibuola and Tambani (Schibuola and Tambani 2021) found high mechanical ventilation rates with efficient air handling units could reduce the risk of infection of COVID-19 and improve energy efficiency in Italian secondary schools. Ben-David and Waring (Ben-David and Waring 2018) studied the effects of increased filtration and ventilation on indoor exposure to PM_{2.5} and ozone. They found that improving filtration tended to have a greater impact on the cost function incorporating energy and exposure costs.

Despite significant recent progress in the literature, there is potential for further analysis. First, studies often assume steady-state scenarios and neglect the dynamics of the HVAC system. For example, constant ventilation rates and outdoor air fractions may be assumed, when these values are dynamic in practice and affect both IAQ and energy consumption. Additionally, researchers often consider energy and costs to quantify sustainability, but do not always include greenhouse gas emissions. This is especially important as new policies incentivize reducing building emissions.

To address this research gap, we propose a study to analyze the tradeoffs between IAQ and costs, including costs associated with filters, HVAC energy consumption, and CO₂ emissions. Newly available dynamic CO₂ emission data is used to quantify emissions in different locations based on electricity sources. Three mitigation strategies are studied in three locations with distinct climates and electricity sources. The mitigation strategies include different levels of filtration, such as MERV 10 and MERV 13 filtration, as well as supply of 100% outdoor air into a building with MERV 10 filtration. We simulate the scenarios using detailed system modeling of a prototype medium office building initially sized for MERV 10 filtration based on the Modelica *Buildings* library (Wetter, Zuo,

¹Department of Mechanical Engineering, University of Colorado Boulder, USA

²Department of Architectural Engineering, University of Colorado Boulder, USA

³Department of Architectural Engineering, Pennsylvania State University, USA

⁴National Renewable Energy Laboratory, USA

⁵Energy Analysis and Environmental Impacts Division, Lawrence Berkeley National Laboratory, USA

et al. 2014; Wetter, Bonvini, et al. 2015). New component models for HVAC filtration and viral transmission are developed to support the analyses in this study.

The remainder of this paper is organized as follows. We describe the Modelica modeling to support the analyses in this study in Section 2. Next, methods to evaluate and compare the mitigation strategies are detailed in Section 3. The scope of analysis for this study including the three mitigation strategies and three locations is described in Section 4. The results in terms of IAQ and costs are presented in Section 5. Finally, conclusions are drawn in Section 6.

2 Modelica Modeling

The modeling based on the Modelica *Buildings* library is detailed in this section. First, we describe the developed component models to support the analyses in this study. We then detail the system modeling of the studied medium office building.

2.1 Component Modeling

We describe the new component models for HVAC filters and viral transmission in this section.

2.1.1 HVAC Filter Model

We first develop an HVAC filter model to simulate filtration of viral particles. The model includes: removal of viral particles based on a defined efficiency and static pressure drop due to the resistance the filter imposes on the airflow.

The removal of virus can be described as:

$$c_{out} = (1 - \eta_{filter})c_{in}, \qquad (1)$$

where c_{out} is the virus concentration exiting the filter, η_{filter} is the filter removal efficiency in terms of percentage of virus removed, and c_{in} is the virus concentration entering the filter. The filter efficiency can be between 0-100%, where η_{filter} = 100% describes a filter that completely removes all virus in the airflow.

Next, the static pressure drop caused by the resistance of the filter is:

$$\Delta p_{filter} = k_{filter} \dot{m}_{filter}^2, \tag{2}$$

where Δp_{filter} is the static pressure drop caused by the filter, \dot{m}_{filter} is the mass flow rate of air though the filter, and k_{filter} is:

$$k_{filter} = \frac{\Delta p_{nom}}{\dot{m}_{nom}^2},\tag{3}$$

where Δp_{nom} is the nominal pressure drop at the nominal mass flow rate, \dot{m}_{nom} . These two values are inputs to the filter model. The quadratic relation between static pressure drop and mass flow rate can be approximated using the Bernoulli equation and captures the general trend from experimental data (ASHRAE 2017). It should be noted

that the filter pressure drop increases over time as the filter collects particles (Xia and Chen 2021), but the nominal pressure drop was assumed to be constant in this study for simplicity.

2.1.2 Viral Transmission Modeling

We use the building level concentration of COVID-19 virus to represent IAQ in the majority of this study. Sick people generate viral particles directly into each well-mixed zone at a constant generation rate. The balance of concentration in a zone can be described as:

$$\dot{c}_{zone} = (1/m_{air,zone})\Sigma(\dot{m}c)_{zone} + \dot{c}_{aen,zone} - \dot{c}_{decay,zone},$$
 (4)

where \dot{c}_{zone} is the rate of change of virus concentration in the zone with respect to time, $m_{air,zone}$ is the mass of air in the zone, $\Sigma(\dot{m}c)_{zone}$ is the net sum of the virus concentration flowrates into/out of the zone, $\dot{c}_{gen,zone}$ is the virus concentration generation rate within the zone, and $\dot{c}_{decay,zone}$ is the rate of viral decay in the zone, which is modeled based on a first order method:

$$\dot{c}_{decay,zone} = k_{decay}c_{zone}, \tag{5}$$

where k_{decay} is a defined constant rate of viral decay, and c_{zone} is the virus concentration in the zone.

The presence of one sick person in each zone within the building is simulated from 9:00 AM - 5:00 PM, Monday through Friday throughout the year. This allows for the evaluation of the mitigation strategies during different conditions, such as weather, throughout the year. The virus generation rate is dependent on many factors, such as the activity level of the sick person. We select a typical virus generation rate of 25 quanta/hr (Buonanno, Stabile, and Morawska 2020; Buonanno, Morawska, and Stabile 2020) and a viral decay rate of 0.48 hr^{-1} (Pease, Wang, et al. 2021) based on data from the literature.

2.2 System Modeling

We provide an overview of the studied medium office building system and modeling of this system in this section.

2.2.1 Studied Building System

The building system in this work is based on the DOE commercial reference medium office building (Department of Energy n.d.), with a focus on the bottom floor. The schematic for this system is shown in Figure 1. The floor consists of five zones, including a core zone and four perimeter zones, with a total floor area of 1,664 m^2 . A central air handling unit with heating and cooling coils services this floor, with VAV terminal boxes containing reheat coils for each zone. An outdoor air economizer is used to supply the minimum outdoor airflow based on ASHRAE standards (ASHRAE 2019) as well as pro-vide free cooling. Natural gas is used to provide heating, while electricity is used to provide cooling and power the

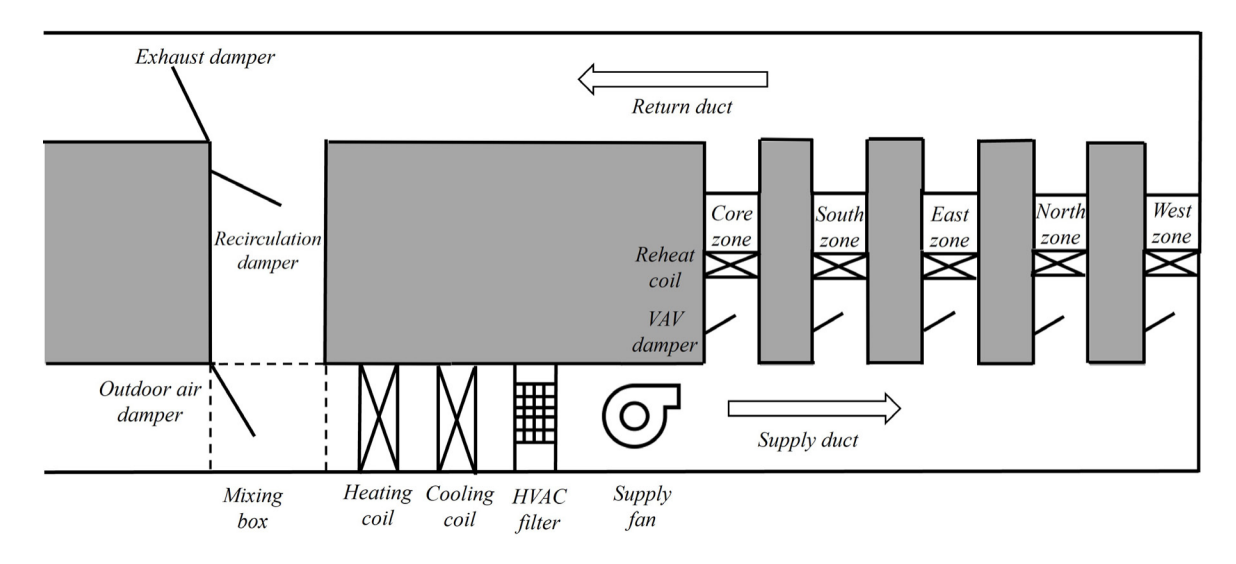


Figure 1. Schematic of VAV system servicing the bottom floor of the five zone medium office building.

fan. The HVAC system is controlled based on the VAV 2A2-21232 sequence from the Sequences of Operation for Common HVAC Systems described in (Wetter, Hu, et al. 2018).

2.2.2 Modeling of Studied System

The new component models are added to a medium office building system model, which is based along a prototype provided in the Modelica Buildings library (Lawrence Berkeley National Laboratory 2013), to create the final modeling capability. The developed medium office building system model for this study is shown in Figure 2. The HVAC system is sized for each climate using EnergyPlusTM and the fan is assumed to be sized for MERV 10 filtration. We use typical meteorological year data for each location (EnergyPlus n.d.). The entire system model contains the following key subsystems: (1) building envelope and room airflow model, including the generation and decay of virus in the zones; (2) HVAC system model which includes the central air handling unit, as well as VAV terminal boxes and return duct: (3) control system, which includes PI controllers for the heating and cooling coils, outdoor air economizer, and supply fan; and (4) the weather conditions, including dry bulb temperature, wind speed, and radiative exchange.

For the system located in Tampa in this study, the model is adapted to supply air through the building at all times, including unoccupied hours to avoid development of mold due to the high humidity. The outdoor air damper is closed during unoccupied hours and only recirculated air is supplied to the building (including for the 100% outdoor air case). For cooling scenarios, the supply air temperature setpoint is reset from 12 °C to 27 °C and the zone temperature setpoints are reset from 24 °C to 30 °C in unoccupied hours. For heating scenarios, the zone temperature setpoints are reset from 20 °C to 12 °C in unoccupied hours. This allows for the system to run and prevent buildup of

mold, while limiting the increase in energy during the unoccupied hours.

3 Methods to Compare Mitigation Strategies

This section describes the methods to compare the mitigation strategies in terms of IAQ and costs. This includes calculating the predicted number of infections based on virus concentration, as well as determining total costs based on costs associated with filters, HVAC energy consumption, and CO₂ emissions.

3.1 Predicted Number of Infections Calculation

To quantify the impact of the virus concentrations, risk of infection is calculated using the Wells-Riley approach (E. Riley, Murphy, and R. Riley 1978), which determines this risk based on the amount of virus inhaled by an occupant. Risk of infection is calculated as:

$$R(t) = 1 - \exp(-IR \sum_{t_0}^{Z} c(t) dt),$$
 (6)

where R(t) is risk of infection in terms of percentage, IR is the volumetric inhalation rate of air for an occupant, and $\frac{R}{t_0}c(t)dt$ is the integral of virus concentration in the room with respect to time since initial time t_0 . The predicted number of infections, R_0 , can be calculated based on the risk, R. The predicted number of infections over time, $R_0(t)$ is calculated accounting for the variable occupancy in the zones for this study. This is done by calculating $R_0(t)$ for a given time interval when the occupancy is constant and adding the predicted number of infections calculated from the previous time interval. This can be described as:

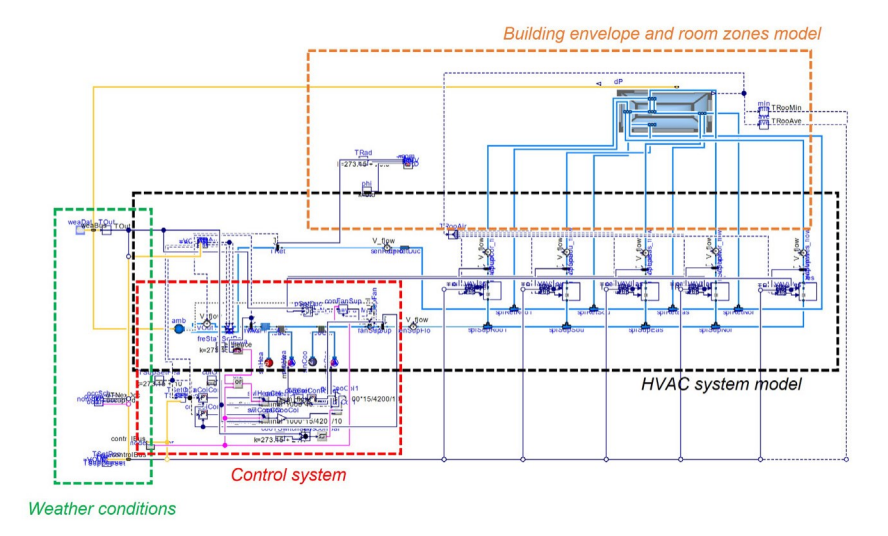


Figure 2. Modelica model of the medium office building system.

$$R_{0,T}(t) = S_T[1 - \exp(-IR \int_{t_0}^{Z} c(t) dt)] + R_{0,T-1}(t_0),$$
 (7)

where $R_{0,T}(t)$ is the predicted number of infections in the zone for time interval T, S_T is the number of susceptible occupants in the zone during T, t_0 is the time at the beginning of interval T, and $R_{0,T-1}(t_0)$ is the predicted number of infections from the previous time interval, T-1, ending at time t_0 . Susceptible occupants is determined as S=N-1, where N is the number of occupants. This way S does not account for the sick person, since they cannot infect themselves.

3.2 Financial Cost Calculation

The annual financial costs for the different mitigation strategies are calculated based on the following equation:

$$J_{total} = J_{filter} + J_{elec} + J_{gas} + J_{CO_2},$$
 (8)

where J_{total} is the total annual costs, J_{filter} are the costs associated with filtration, J_{elec} are the electricity costs to run the HVAC system, Jgas are the costs for natural gas heating, and J_{CO_2} are costs associated with CO_2 emissions. The costs associated with filtration include purchase costs and labor costs for replacing the filters throughout the year based on their expected life. The electricity costs to run the HVAC system come from fan and cooling power, while natural gas costs are calculated based on the heat supplied in the HVAC system from natural gas. Finally, we use a cost of \$12 (USD) per ton of CO2 emissions based on average prices in the U.S. described by the Regional Greenhouse Gas Initiative and California Cap-and-Trade Program (The World Bank 2021) to determine costs associated with CO_2 emissions. It should be noted J_{filter} , J_{elec} , and J_{gas} are charged in current practice, but J_{CO} has not been implemented in the building sector in the United States yet.

3.3 CO₂ Emissions Calculation

The annual CO₂ emissions for the mitigation strategies are determined based on emissions associated with natural gas heating and electricity consumed by the HVAC system, using the method adopted in (Lou, Yang, et al. 2021; Lou, Ye, et al. 2022). The emission factor for natural gas heating is constant and independent of location. However, the emission factor for electricity is dynamic and depends on the electricity sources of the location. Different locations use various portions of renewable, nuclear, or fossil fuel energy. The electricity sources vary based on the time of day as well as season, for example depending on the availability of solar or wind energy. The emission factor data comes from the Cambium project lead by the National Renewable Energy Laboratory (Gagnon et al. 2020).

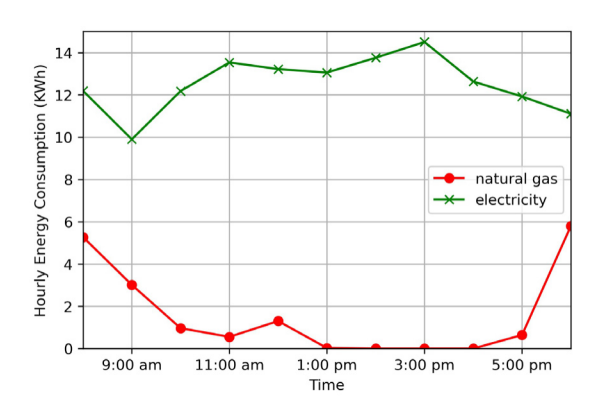
Figure 3 shows an example of how CO_2 emissions are calculated for a sample day based on the natural gas and electricity usage. Figure 3a shows the energy consumption for one heating day in San Diego. We see the natu-ral gas usage varies based on the heating demand and the electricity consumption changes based on the fan power. The emission factor of electricity in Figure 3b varies during the day based on the availability of renewable energy, while the emission factor of natural gas remains constant. Finally, Figure 3c shows the hourly CO_2 emissions are the product of the hourly energy usage and emission factor.

3.4 Analysis of Combined Metrics

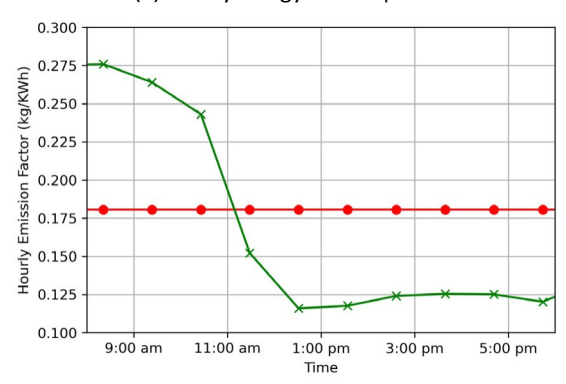
To evaluate the performance of the two strategies relative to MERV 10 filtration, we define metrics to consider the improvement in IAQ relative to an increase in costs. These are relative metrics, since they are calculated for the strategies relative to MERV 10 filtration. First, we calculate the percent increase in costs relative to MERV 10 filtration. This is described as:

$$\Delta J_i = J_i / J_{M10} - 1,$$
 (9)

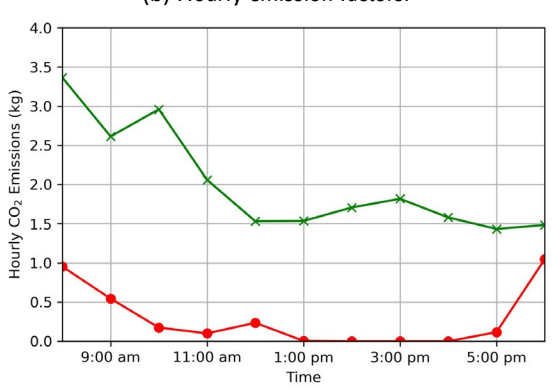
where ΔJ_i is the percent increase in costs associated with a strategy i relative to MERV 10 filtration, J_i is the costs for strategy i, and J_{M10} is the costs for MERV 10 filtration in that location.



(a) Hourly energy consumption.



(b) Hourly emission factors.



(c) Hourly CO2 emissions.

Figure 3. Calculation of CO_2 emissions based on electricity and natural gas usage for Jan 1, 2020 in San Diego.

The percent improvement in IAQ relative to the percent increase in costs can then be calculated as:

$$\Delta IAQ/\Delta J_i = (1 - IAQ_i/IAQ_{M10})/\Delta J_i, \qquad (10)$$

where $\Delta IAQ/\Delta J_i$ is the marginal improvement in IAQ per increase in costs for a strategy i relative to MERV 10 filtration, IAQ_i is the IAQ metric for a strategy i, and IAQ_{M10} is the IAQ metric for the MERV 10 strategy.

4 Scope

We describe the scope of our analysis in this section, including the selected mitigation strategies and summary of the chosen geographic locations.

4.1 Mitigation Strategies

Three mitigation strategies are chosen for this study, including use of MERV 10 and MERV 13 filtration, or supply of 100% outdoor air into the building. MERV 10 filtration may be used in existing buildings, while improved MERV 13 filtration has been recommended for use during the COVID-19 pandemic by ASHRAE (ASHRAE Epidemic Task Force 2021). The 100% outdoor air strategy also uses MERV 10 filtration, since filtration is needed for outdoor contaminants as well. This study assumes the viral particles have diameters between 1-3 μm , and a constant, typical removal efficiency is chosen based on filter data for particles of this size. Table 1 shows the settings for the HVAC filters used in the simulations. The filtration efficiencies come from ASHRAE technical resources (ASHRAE 2017) and the pressure drop values come from data for MERV 10 (Dwyer n.d.[a]) and MERV 13 (Dwyer n.d.[b]). It should be noted the pressure drop across the filter can increase over time as the filter accumulates particles (Xia and Chen 2021) and the pressure drop can vary for filters with the same rating, depending on the depth or type of filter (Ben-David and Waring 2018). For simplicity, a constant nominal pressure drop for each filter is chosen based on the average of the typical initial and final pressure drops.

Table 1. HVAC filter simulation settings.

Filter	Nominal Pressure Drop (Pa)	Filtration Efficiency
MERV 10 MERV 13	143 162	50% 85%

The costs of the HVAC filters, which are obtained from (Azimi and Stephens 2013), are shown in Table 2. The total annual costs are determined by the purchase and labor costs throughout the year based on the expected life of the filters.

4.2 Studied Locations

International Falls, MN, San Diego, CA, and Tampa, FL are the locations studied in this paper. A summary of the climates, electricity sources, energy prices, and average electricity emission factor is shown in Table 3. The electricity (U.S. Energy Information Administration 2021b)

Table 2. HVAC filter costs.

Filter	Cost	Replacement Labor Costs (USD)	Expected Life	Total Annual Costs
MERV 10	\$7	\$17	4 months	\$72
MERV 13	\$11	\$17	4 months	\$84

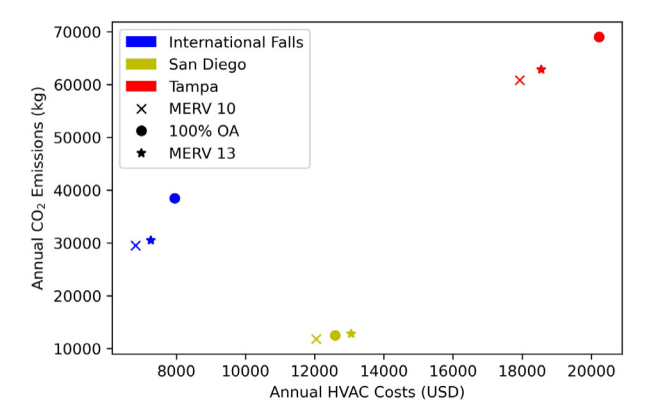
and natural gas (U.S. Energy Information Administration 2021a) prices for each location are also included. The natural gas price is based on the total price paid by endusers per thousand cubic feet of natural gas, and is inclusive of all taxes and other fees. Compared to International Falls and Tampa, San Diego has a lower average electricity emission factor. San Diego is able to utilize significant renewable energy, such as solar power, and limit its fos-sil fuel usage. International Falls and Tampa instead rely more on fossil fuels such as coal and natural gas for electricity generation.

5 Results and Discussion

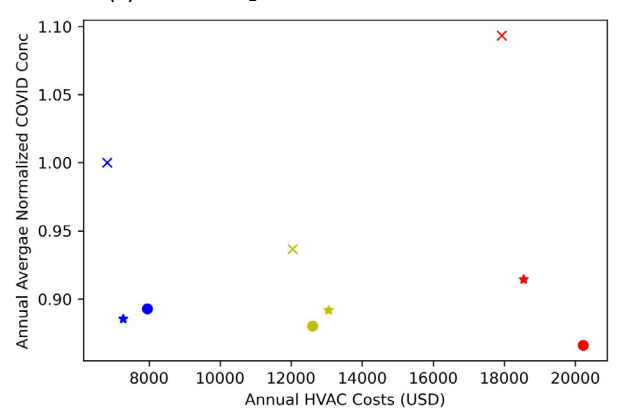
We first show an overview of the results for the three mitigation strategies in the three locations in terms of IAQ, HVAC costs, and $\rm CO_2$ emissions. We then discuss the tradeoffs between IAQ and totals costs.

5.1 Overview of Results

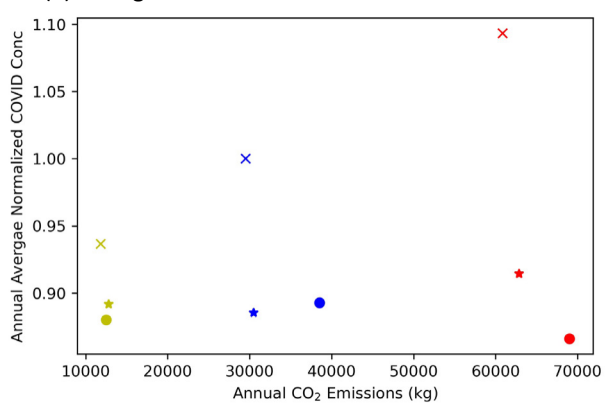
The annual results for IAQ, HVAC costs, and CO₂ emissions are shown in Figure 4. The virus concentrations are normalized by the annual average virus concentration for the MERV 10 case in International Falls. The HVAC costs in this section include costs associated with filters and HVAC energy consumption, while the total costs including those associated with CO₂ emissions are used in the next section. The results show dependencies on mitigation strategy, climate, and electricity sources. The trends for emissions and costs can be seen in Figure 4a. San Diego has lower costs and emissions compared to Tampa, due to less HVAC energy consumption in the milder climate. The breakdown of HVAC energy consumption for the three mitigation strategies in the three locations is shown in Figure 5. International Falls has lower costs but more emissions compared to San Diego. This is because natural gas heating is the dominant energy consumption in the very cold climate of International Falls, which has much lower costs compared to electricity. Due to its climate, San Diego uses very little heating and most of the HVAC energy consumption comes from electricity to provide cooling and power the fan. The lower emissions in San Diego compared to International Falls can be explained by the lower HVAC energy consumption, as well as the lower average electricity generation emission factor.



(a) Annual CO₂ emissions vs HVAC costs.



(b) Average virus concentration vs annual HVAC costs.



(c) Average virus concentration vs annual CO₂ emissions.

Figure 4. Results for average virus concentration, annual HVAC costs, and annual CO_2 emissions for the three mitigation strategies in the three locations.

Table 3. Summary of selected locations.

Location	Climate	Electricity Price (cents/kWh)	Natural Gas Price (cents/kWh)	Avg. Electricity Emission Factor (kg CO ₂ /MWh)
International Falls, MN	Very Cold	10.57	2.18	302
San Diego, CA	Warm and Marine	18.00	3.34	196
Tampa, FL	Hot and Humid	10.06	3.93	338

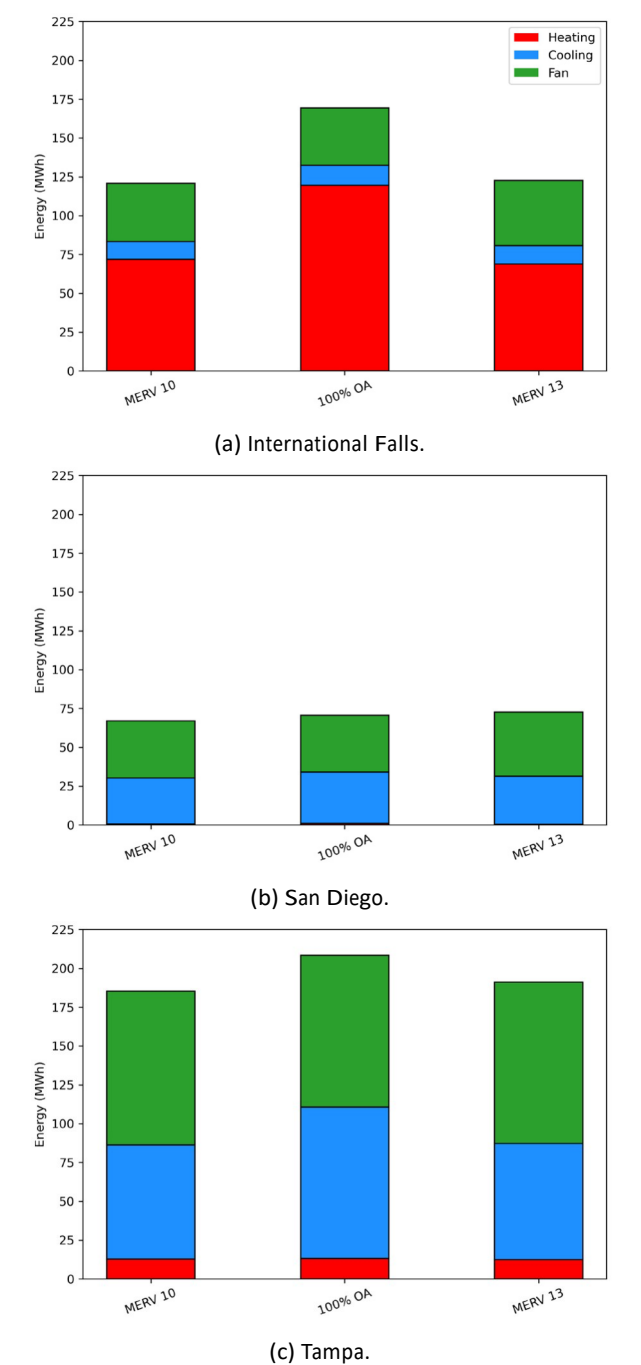
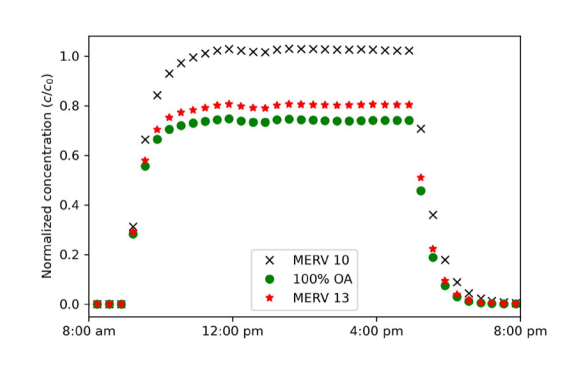
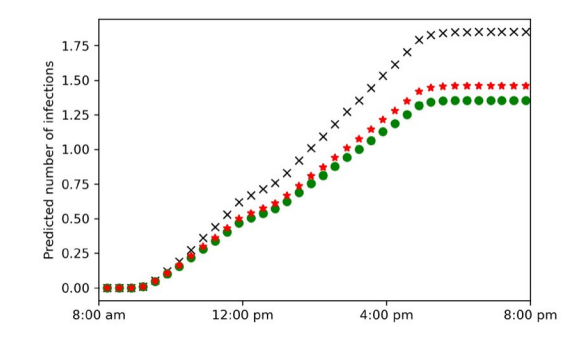


Figure 5. Breakdown of HVAC energy consumption for the three strategies in the three locations.



(a) Virus concentration.



(b) Predicted number of infections.

Figure 6. Virus concentration and predicted number of infections in the Core zone for the three strategies on June 24, 2020 in Tampa.

Figures 4b and 4c similarly show the trends based on climate and electricity sources, as well as the IAQ trends for the different mitigation strategies. The 100% outdoor air strategy provides the best IAQ in Tampa and San Diego, but not in International Falls. This is because the economizer only decreases the outdoor air usage for the 100% outdoor air strategy when it is very cold outside to prevent freezing, which happens more often in the very cold climate of International Falls. The 100% outdoor air strategy leads to significant increases in costs and CO2 emissions in International Falls and Tampa, but not as significantly in San Diego. This is because significant energy is required either to cool and dehumidify the outdoor air in the hot and humid Tampa climate or to heat the very cold outdoor air in International Falls. In San Diego, however, the weather is milder throughout the year, so the 100%

outdoor air strategy leads to smaller increases in costs and emissions. Figure 5 shows the increase in energy consumption for the 100% outdoor air case in Tampa and International Falls, as well as overall higher energy consumption in these two locations compared to San Diego because of climate.

To compare the impact of the differences in virus concentrations for these strategies, an example of the virus concentration and predicted number of infections in the Core zone for a hot summer day (June 24, 2020) in Tampa is shown in Figure 6. The minimum outdoor airflow is used for the MERV 10 and MERV 13 cases on this day. Use of MERV 13 filtration reduces the peak virus concentration on this day by 22% compared to MERV 10 filtration, and use of 100% outdoor air reduces the peak virus concentration by 27% compared to MERV 10 filtration. The predicted number of infections is above one for all three strategies in this zone during this day, which means at least one infection is expected to occur. MERV 13 filtration reduces the expected chance of a second infection occurring by 39% compared to MERV 10 filtration, while supply of 100% outdoor air decreases the expected chance of a second infection occurring by 50% compared to MERV 10 filtration.

MERV 10 filtration is the cheapest and lowest emission strategy due to having the lowest energy consumption, but also provides the worst IAQ in all locations. MERV 13 filtration improves the IAQ relative to MERV 10 filtration, but with moderate increases in costs and emissions because of the increase in fan energy consumption. It can be seen that the improvement in IAQ for the other strategies relative to MERV 10 filtration differs between the two locations. Additionally, the costs and emissions for the mitigation strategies also differ for these locations. Analysis of these tradeoffs is performed in the following section.

5.2 Analysis of Tradeoffs

The tradeoffs between IAQ and costs for the mitigation strategies relative to MERV 10 filtration are analyzed for the three locations in this section. Associating a cost with CO_2 emissions allows us to directly compare the marginal improvement in IAQ to both costs and emissions simultaneously, as described in Section 3.4. This is shown for the two strategies relative to MERV 10 in the three locations in Figure 7.

Use of 100% outdoor air outperforms MERV 13 filtration in San Diego. This is because supply of 100% outdoor air is able to provide better IAQ compared to MERV 13 with less of an increase in costs in this location. The milder weather in San Diego allows for limited increases in heating/cooling costs throughout the year, while the increase in fan energy for the MERV 13 case slightly increases the overall costs compared to 100% outdoor air. On the other hand, MERV 13 filtration appears to be the most beneficial strategy in International Falls and Tampa. Unlike San Diego, use of 100% outdoor air significantly increases the costs due to the energy required to

heat or cool and dehumidify the outdoor air in these locations. MERV 13 filtration also shows a more significant improvement in IAQ in the two locations relative to San Diego due to the limited amount of outdoor air usage in those climates.

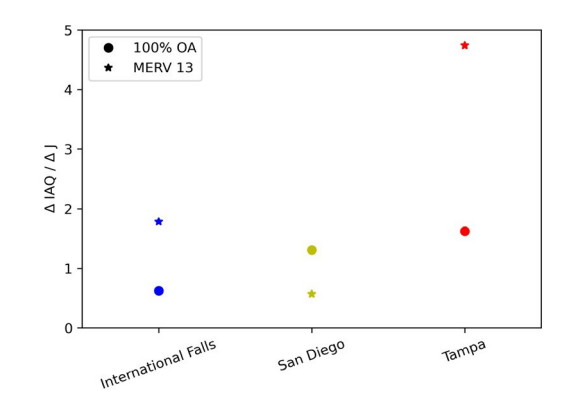


Figure 7. Marginal improvement in IAQ relative to total costs for the three locations.

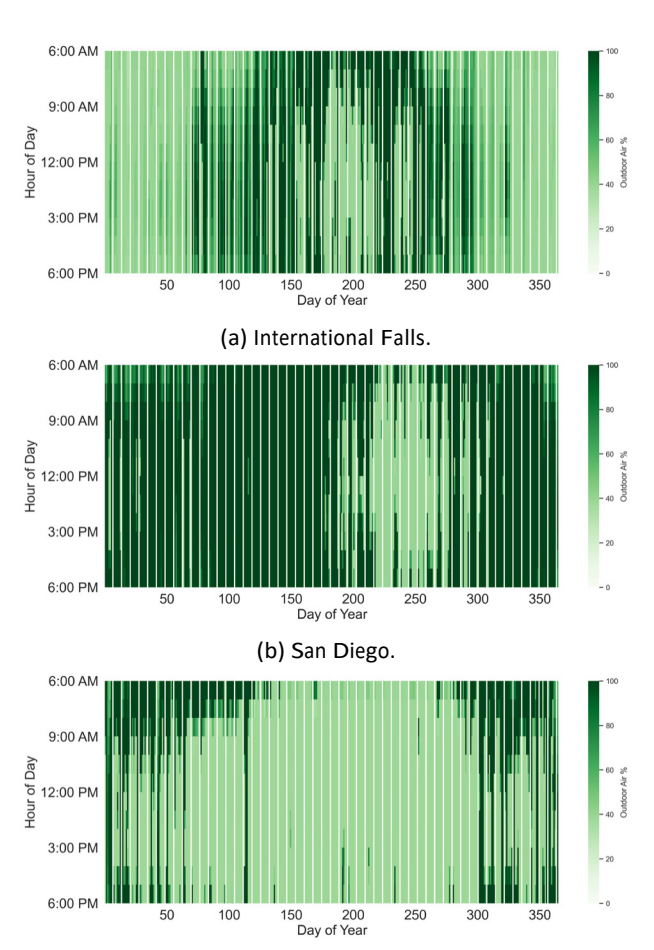


Figure 8. Dynamic usage of outdoor air using MERV 10 filtration in the three locations.

(c) Tampa.

Figure 8 shows the outdoor air usage for the MERV 10 cases in the three locations. Because of its milder weather, the MERV 10 case in San Diego can use high outdoor airflow rates most of the year, except in the peak of summer in July - September. In International Falls, the MERV 10 case uses less outdoor air during the very cold winter, as well as during the peak of summer around July. In Tampa, much less outdoor air is used for the MERV 10 case throughout the year, with an exception during the cooler winter mornings. Because of these trends for the MERV 10 cases, the additional filtration in the MERV 13 case or outdoor air usage in the 100% outdoor air case significantly improves the IAQ in International Falls and Tampa.

6 Conclusion

The tradeoffs between IAQ and sustainability for three strategies to mitigate indoor virus are compared for three locations in the United States. The mitigation strategies include different levels of filtration, such as MERV 10 or MERV 13 filtration, as well as supply of 100% outdoor air into the building. The locations have differing climates and their electricity profiles are also comprised with varying portions of renewable energies and fossil fuels for generating electricity. The strategies are evaluated using a prototypical medium office building model initially sized for MERV 10 filtration, developed using the Modelica *Buildings* library.

The results show the tradeoffs between IAQ and costs for the different strategies have a strong dependency on climate and electricity sources. MERV 10 filtration is always the cheapest option, since this strategy tends to use the least energy, but also provides the worst IAQ. Use of 100% outdoor air provides the best IAQ in San Diego and Tampa, and significantly increases costs in the hot and humid climate of Tampa and very cold climate of International Falls. Use of 100% outdoor air can be a good option in the relatively milder climate of San Diego, where the increase in costs and emissions is limited. MERV 13 filtration can improve IAQ with limited increases in costs in all locations due to its high virus filtration efficiency and relatively smaller increases in energy consumption. This strategy outperforms use of 100% outdoor air in International Falls and Tampa, since it avoids the significant increase in cooling/dehumidification or heating of the outdoor air.

Future studies can be conducted based on the work in this paper. The models we used in this study can be applied to other contaminant scenarios, for example PM_{2.5} which can infiltrate the building from outdoor air. They can also be used to evaluate advanced control strategies to improve IAQ, such as occupant-based strategies. Finally, this study focuses on applying mitigation strategies to an existing building, since redesigning an HVAC system is costly. However, the models can be used to evaluate HVAC system designs for new buildings, for example to study a system designed for high-efficiency filters.

Acknowledgements

This research was supported in part by the U.S. Defense Threat Reduction Agency and performed under U.S. Department of Energy Contract No. DE-AC02-05CH11231. This work emerged from the IBPSA Project 1, an international project conducted under the umbrella of the International Building Performance Simulation Association (IBPSA). Project 1 will develop and demonstrate a BIM/GIS and Modelica Framework for building and community energy system design and operation. This research was supported by the National Science Foundation under Awards No. CBET-2217410.

References

ASHRAE (2017). "Standard 52.2. Method of Testing General Ventilation Air-Cleaning Devices for Removal Efficiency by Particle Size". In: American Society of Heating, Refrigerating and Air-Conditioning Engineers.

ASHRAE (2019). "Standard 62.1 Ventilation for Acceptable Indoor Air Quality". In: *American Society of Heating, Refrigerating and Air-Conditioning Engineers*.

ASHRAE Epidemic Task Force (2021). "Core Recommendations for Reducing Airborne Infectious Aerosol Exposure". In: ASHRAF.

Aviv, Dorit et al. (2021). "A fresh (air) look at ventilation for COVID-19: Estimating the global energy savings potential of coupling natural ventilation with novel radiant cooling strategies". In: *Applied Energy* 292, p. 116848.

Azimi, Parham and Brent Stephens (2013). "HVAC filtration for controlling infectious airborne disease transmission in indoor environments: predicting risk reductions and operational costs". In: *Building and environment* 70, pp. 150–160.

Ben-David, Tom and Michael S Waring (2018). "Interplay of ventilation and filtration: Differential analysis of cost function combining energy use and indoor exposure to PM_{2.5} and ozone". In: *Building and Environment* 128, pp. 320–335.

Buonanno, Giorgio, Lidia Morawska, and Luca Stabile (2020). "Quantitative assessment of the risk of airborne transmission of SARS-CoV-2 infection: prospective and retrospective applications". In: *Environment international* 145, p. 106112.

Buonanno, Giorgio, Luca Stabile, and Lidia Morawska (2020). "Estimation of airborne viral emission: Quanta emission rate of SARS-CoV-2 for infection risk assessment". In: *Environment international* 141, p. 105794.

Cortiços, Nuno D and Carlos C Duarte (2021). "COVID-19: The impact in US high-rise office buildings energy efficiency". In: *Energy and Buildings* 249, p. 111180.

Department of Energy (n.d.). Commercial Reference Buildings. https://www.energy.gov/eere/buildings/commercial-reference-buildings.

Dwyer (n.d.[a]). MERV 10 Pleated Filters. https://www.dwyer-inst.com/PDF_files/Priced/DF10_cat.pdf.

Dwyer (n.d.[b]). MERV 13 Pleated Filters. https://www.dwyer-inst.com/PDF files/Priced/DF13 cat.pdf.

EnergyPlus (n.d.). Weather Data. https://energyplus.net/

Faulkner, Cary A et al. (2022). "Investigation of HVAC operation strategies for office buildings during COVID-19 pandemic". In: *Building and Environment* 207, p. 108519.

- Gagnon, Pieter et al. (2020). Cambium data for 2020 Standard Scenarios. National Renewable Energy Laboratory. https://cambium.nrel.gov/.
- Lawrence Berkeley National Laboratory (2013). *Build-ings.Examples.VAVReheat*. https://simulationresearch.lbl.gov/modelica/releases/v5.0.0/help/Buildings_Examples_VAVReheat.html#Buildings.Examples.VAVReheat.
- Lou, Yingli, Yizhi Yang, et al. (2021). "The effect of building retrofit measures on CO2 emission reduction—A case study with US medium office buildings". In: *Energy and Buildings* 253, p. 111514.
- Lou, Yingli, Yunyang Ye, et al. (2022). "Long-term carbon emission reduction potential of building retrofits with dynamically changing electricity emission factors". In: *Building and Environment* 210, p. 108683.
- Pease, Leonard F, Timothy I Salsbury, et al. (2022). "Size dependent infectivity of SARS-CoV-2 via respiratory droplets spread through central ventilation systems". In: *International Communications in Heat and Mass Transfer* 132, p. 105748.
- Pease, Leonard F, Na Wang, et al. (2021). "Investigation of potential aerosol transmission and infectivity of SARS-CoV-2 through central ventilation systems". In: *Building and Environment* 197, p. 107633.
- Riley, EC, G Murphy, and RL Riley (1978). "Airborne spread of measles in a suburban elementary school". In: *American journal of epidemiology* 107.5, pp. 421–432.
- Santos, Hugo RR and Vitor MS Leal (2012). "Energy vs. ventilation rate in buildings: A comprehensive scenario-based assessment in the European context". In: *Energy and Buildings* 54, pp. 111–121.
- Schibuola, Luigi and Chiara Tambani (2021). "High energy efficiency ventilation to limit COVID-19 contagion in school environments". In: *Energy and Buildings* 240, p. 110882.
- Shen, Jialei et al. (2021). "A systematic approach to estimating the effectiveness of multi-scale IAQ strategies for reducing the risk of airborne infection of SARS-CoV-2". In: *Building and environment* 200, p. 107926.
- The World Bank (2021). Carbon Pricing Dashboard. https://carbonpricingdashboard.worldbank.org/map_data.
- U.S. Energy Information Administration (2021a). *Natural Gas Prices*. https://www.eia.gov/dnav/ng/ng_pri_sum_a_EPG0_PCS_DMcf_a.htm.
- U.S. Energy Information Administration (2021b). *State Electricity Profiles*. https://www.eia.gov/electricity/state/.
- Vlachokostas, Alex et al. (2022). "Experimental evaluation of respiratory droplet spread to rooms connected by a central ventilation system". In: *Indoor air*.
- Wetter, Michael, Marco Bonvini, et al. (2015). "Modelica buildings library 2.0". In: Proc. of The 14th International Conference of the International Building Performance Simulation Association (Building Simulation 2015), Hyderabad, India.
- Wetter, Michael, Jianjun Hu, et al. (2018). "OpenBuildingControl: Modeling feedback control as a step towards formal design, specification, deployment and verification of building control sequences". In: Building Performance Modeling Conference and SimBuild.
- Wetter, Michael, Wangda Zuo, et al. (2014). "Modelica buildings library". In: *Journal of Building Performance Simulation* 7.4, pp. 253–270.
- Xia, Tongling and Chun Chen (2021). "Evolution of pressure drop across electrospun nanofiber filters clogged by solid particles and its influence on indoor particulate air pollution control". In: Journal of Hazardous Materials 402, p. 123479.